

Tryptophan-containing lipopeptide antibiotics derived from polymyxin B with activity against Gram positive and Gram negative bacteria.

Ariadna Grau-Campistany^{a,b}, Ángeles Manresa^c, Montserrat Pujol^{a,d}, Francesc Rabanal^b, Yolanda Cajal^{a,d*}

^aDepartment of Physical Chemistry, Faculty of Pharmacy, University of Barcelona, Joan XXIII s/n, 08028 Barcelona, Spain;

^bDepartment of Organic Chemistry, Faculty of Chemistry, University of Barcelona, Martí i Franquès 1, 08028 Barcelona, Spain;

^cLaboratory of Microbiology, Faculty of Pharmacy, University of Barcelona, Joan XXIII s/n, 08028 Barcelona, Spain; ^dNanociencia and Nanotechnology Institute IN2UB.

*Tel: +34-3-4024553 Email: ycajal@ub.edu (Y. Cajal)

ABSTRACT

Resistance to all known antibiotics is a growing concern worldwide, and has renewed the interest in antimicrobial peptides, a structurally diverse class of amphipathic molecules that essentially act on the bacterial membrane. Propelled by the antimicrobial potential of this compound class, we have designed three new lipopeptides derived from polymyxin B, sp-34, sp-96 and sp-100, with potent antimicrobial activity against both Gram positive and Gram negative bacteria. The three peptides bind with high affinity to lipopolysaccharide as demonstrated by monolayer penetration and dansyl-displacement. The interaction with the cytoplasmic membrane has been elucidated by biophysical experiments with model membranes of POPG or POPE/POPG (6:4), mimicking the Gram positive and Gram negative bacterial membrane. Trp-based fluorescence experiments including steady-state, quenching, anisotropy and FRET, reveal selectivity for anionic phospholipids and deep insertion into the membrane. All three lipopeptides induce membrane fusion and leakage from anionic vesicles, a process that is favored by the presence of POPE. The molecules bind to zwitterionic POPC vesicles, a model of the eukaryotic membrane, but in a different way, with lower affinity, less penetration into the bilayer and no fusion or permeabilization of the membrane. Results in model membranes are consistent with flow cytometry experiments in *Escherichia coli* and *Staphylococcus aureus* using a membrane potential sensitive dye (bis-oxonol) and a nucleic acid dye (propidium iodide), suggesting that the mechanism of action is based on membrane binding and collapse of membrane integrity by depolarization and permeabilization.

1. Introduction

Disease-causing microbes that have become resistant to antibiotic drug therapy are an increasing public health concern [1,2]. Part of the problem is that bacteria are remarkably resilient and have developed several ways to resist antibiotics. However, the main reason is our increasing use, and misuse, of existing antibiotics in human and veterinary medicine and in agriculture. Unless antibiotic resistance problems are detected as

they emerge, and actions are taken immediately to contain them, society could be faced with previously treatable diseases that have become again untreatable, as in the pre-antibiotic era. In particular there is substantial concern worldwide with the mounting prevalence of infections caused by multidrug-resistant bacteria, including methicillin-resistant *Staphylococcus aureus*, vancomycin-resistant enterococci, and certain Gram negative bacteria such as *Pseudomonas aeruginosa*, *Acinetobacter baumannii* and *Klebsiella pneumoniae* [3]. Conventional antibiotics typically interact with one or more specific target protein or receptor, and genetic resistance appears at a rate that depends on many factors, such as the number of targets. These phenomena have led to intensive efforts aimed at the development of novel drugs targeting the bacterial cell membranes, such as antimicrobial peptides (AMP's). AMP's offer a new class of therapeutic agents to which bacteria may not be able to develop genetic resistance, since they act on the lipid component of the cell membranes [4,5]. Among these compounds, polymyxin B (PxB) is acquiring new therapeutical relevance and is starting to be considered as a representative of a new class of antibiotics against multiresistant bacteria [6,7]. PxB and other members of the polymyxin family such as colistin are drugs of last resort to treat Gram negative multiresistant infections [8,9]. In addition, resistance to polymyxins is rare, and generally adaptive and thus reversible. PxB is also capable of inhibiting the biological activities of bacterial lipopolysaccharide (LPS) through high-affinity binding to the lipid A moiety, being the agent of choice to treat septic shock. Considering the above, there is no doubt on the importance of developing new molecules that maintain or improve the activity of polymyxins and at the same time present lower toxicity. The mechanism of action of PxB is not based on a detergent or lytic effect on the membrane, as it was previously thought. Biophysical studies using model membranes have demonstrated that PxB induces the apposition of anionic vesicles and the formation of functional vesicle-vesicle contacts that support a fast and selective exchange of phospholipids exclusively between the outer monolayers of the vesicles, maintaining intact the inner monolayers and the aqueous contents [10,11]. This biophysical phenomena has been proposed as the mechanism of antibacterial action of PxB and several other antibiotic peptides [12,13].

In this paper we describe new cationic lipopeptides based on the structure of the Gram negative selective antimicrobial PxB that show activity against both Gram positive and Gram negative bacteria. PxB, as most basic nonribosomal peptides, is a complex molecule to approach synthetically. We have previously described the synthesis and biophysical activity of sp-B [14,15], an analogue that keeps the basic features of PxB that are important for activity. Biophysical studies have shown that sp-B interaction with phospholipid vesicles is analogous to the interaction of PxB. Both PxB and sp-B bind selectively to anionic membranes and induce the formation of vesicle-vesicle contacts and selective lipid exchange. Based on this lipopeptide, we have designed a series of more than 100 analogues with different substitutions, and tested their

antibacterial activity [16]. From these results, we have selected three lipopeptide analogues, sp-34, sp-96, and sp-100 (structures in Table 1), that show broad spectrum activity. The three compounds share a (D)-tryptophan in position 7, replacing (D)-phenylalanine, thus conferring the molecules intrinsic fluorescence. In addition, several key Dab residues are mutated to Arginine. Other modifications include a (D)-cysteine in position 10 (sp-96 and sp-100), and Norleucine instead of Leu⁷ (sp-100). The influence of the lipid tail is also explored by including either C9 or C10 acyl chain in the N-terminus. The rationale for these modifications is summarized in the Discussion section of this work. We have determined the antimicrobial activity on Gram positive and Gram negative bacteria, and analyzed the interaction with lipid vesicles with a composition strategically designed to simulate the outer leaflet of cell membranes. Our goal was to see which role interactions with the lipid matrix of the target membranes play in the biological effects. Unilamellar vesicles of POPG or a mixture POPE/POPG (6:4) were used. In general, higher amounts of PEs are found in Gram negative bacteria, whereas Gram positive bacteria are better modeled with PG [17]. LPS vesicles and monolayers represent the outer leaflet of the Gram negative outer membrane. Zwitterionic POPC vesicles were used to mimic the eukaryotic membrane, as a first approach to detect peptide specificity. We found a good correlation between the biophysical studies on model membranes and the antimicrobial activity *in vitro*. The interaction of these molecules with model membranes is consistent with a membrane-based mechanism of action, with high specificity for anionic lipids. Destabilization of the bacterial membrane is directly observed by flow cytometry in *E. coli* and *S. aureus*.

2. Materials and methods

2.1. Materials

Polymyxin B sulfate salt (PxB), lipopolysaccharide (LPS) from *Salmonella enterica* serotype minnesota Re 595 (Re mutant), bis-(1,3-dibutylbarbituric acid) trimethine oxonol (DiBAC₄ (3) or BOX), acrylamide and Trizma base (Tris), were purchased from Sigma-Aldrich (St Louis, MO). 1-palmitoyl-2-oleoyl-glycero-*sn*-glycero-3-phospho-(1'-*rac*-glycerol) (POPG), 1-palmitoyl-2-oleoyl-*sn*-glycero-3-phosphoethanolamine (POPE), and 1-palmitoyl-2-oleoyl-*sn*-glycero-3-phosphocholine (POPC) were from Avanti Polar Lipids (Alabaster, Ala). N-(7-nitro-2-(1,3-benzoxadiazol-4-yl) dioleoylphosphatidylethanolamine (NBD-PE), 1-hexadecanoyl-2-(1-pyrenedecanoyl) glycero-*sn*-3-phospho-(1'-*rac*-glycerol) (pyPG), 1-hexadecanoyl-2-(1-pyrenedecanoyl) glycero-*sn*-3-phosphocholine (pyPC), 1-aminonaphthalene-3,6,8-trisulfonic acid (ANTS), *N,N*-*p*-xylenebis(pyridinium bromide) (DPX), propidium iodide (PI), and dansyl-polymyxin B were purchased from Invitrogen Molecular Probes (Eugene, OR). *N*-fluorenylmethoxycarbonyl (Fmoc)-protected amino acids, *N,N*-diisopropylcarbodiimide (DIPCDI), *N*-hydroxybenzotriazole (HOBt), trifluoroacetic acid (TFA) as well as

nonanoic and decanoic acids were from Bachem and Fluka (Switzerland). Rink amide resin was purchased from Novabiochem (Läufelfingen, Switzerland). Water was doubly distilled and deionized (Milli-Q system, Millipore Corp.). All the lipopeptides were used as water solutions and the concentration was determined by quantitative amino acid analysis.

2.2. Lipid vesicles

Unilamellar vesicles of POPG, POPE/POPG (6:4) or POPC, alone or with the fluorescently labeled phospholipids: pyPG, pyPC or NBD-PE, were prepared by evaporation of a mixture of the lipids and probes in $\text{CHCl}_3/\text{CH}_3\text{OH}$ (2:1 v/v). The dried film was hydrated for a final lipid concentration of 10 mM, and then sonicated in a bath type sonicator (Lab Supplies, Hicksville, NY, Model G112SPIT) until a clear dispersion was obtained (2-4 minutes). For the ANTS/DPX fusion assay, the dried lipid films were dispersed in 12.5 mM ANTS, 45 mM DPX and 10 mM Tris pH 8.0 and subjected to 10 freeze-thaw cycles prior to extrusion 10 times through a 0.1 μm polycarbonate membrane at 250 psi N_2 pressure (LIPEX, Northern Lipids Inc.). The unencapsulated material was separated by gel-filtration on a Sephadex G-50 column eluted with 10 mM Tris 80 mM NaCl. Osmolarities were adjusted with NaCl and measured in an osmometer (3320 Osmometer, Advanced Instruments Inc.). Lipid phosphorus was determined by the Stewart-Marshall assay. These vesicles were used within 10 h. Vesicle size was measured by dynamic light scattering with a Malvern II-C autosizer, typically obtaining a mean diameter of 80 nm and 105 nm for sonicated and extruded respectively, and a narrow size distribution (polydispersity < 0.1).

2.3. Peptide synthesis and purification

Peptide synthesis was performed manually following standard Fmoc/^tBu procedures using DIPCDI/HOBt activation on a Rink amide resin [18]. Once the sequence was assembled, cleavage of the peptides from the resin was carried out by acidolysis with TFA:triisopropylsilane:water (95:3:2, v/v) for 90 minutes. TFA was removed with N_2 stream and the oily residue was treated with dry diethyl ether to obtain the peptide precipitate. The solid peptide was isolated by centrifugation. This process was repeated three times. Homogeneity of peptide crudes was assessed by analytical HPLC using Nucleosil C18 reverse phase columns (4 x 250 mm, 5 μm particle diameter, 120 Å porous). Elution was carried out at 1 ml·min⁻¹ flow with mixtures of H_2O -0.045% TFA and acetonitrile-0.036% TFA and UV detection at 220 nm. Peptides were purified by preparative HPLC on a Waters Delta Prep 3000 system using a Phenomenex C18 (2) column (250 x 10 mm, 5 μm) eluted with H_2O -acetonitrile-0.1% TFA gradient mixtures and UV detection at 220 nm. Cyclization of peptides through disulfide bonds was carried out in 100 mM ammonium bicarbonate aqueous solutions with a pH adjusted to 10 by addition of aqueous concentrated ammonia (32%). Final purity was

greater than 95%. Peptides were characterized by amino acid analysis with a Beckman 6300 analyzer and by MALDI-TOF with a Bruker model Biflex III.

2.4. Determination of antibacterial activity

The minimal inhibitory concentrations (MIC) against *Escherichia coli* (ATTC 25922) and *Staphylococcus aureus* (ATTC 29213) were determined by the broth microdilution method [19] in Mueller-Hinton broth in 96-well polypropylene microtiter plates with a final concentration of 10^5 CFU/mL. The MIC was determined as the lowest peptide concentration at which growth was completely inhibited after overnight incubation of the plates at 37°C.

2.5. Dansyl-PxB binding and displacement assay.

The relative binding affinity of each peptide for LPS was determined using the dansyl-polymyxin B displacement assay [20], based on the fact that the dansyl group fluoresces when located within a hydrophobic lipid environment, whereas it undergoes self-quenching in aqueous solution following displacement by membrane-bound species. Fluorescence was measured using a PTI QM4 spectrofluorimeter with excitation of 340 nm and emission of 485 nm. The saturation of LPS was determined by recording the fluorescence after the addition of portions of dansyl-polymyxin to a 1 mL cuvette containing 3 µg/mL of LPS in 10 mM Tris buffer (pH 8.0). The background fluorescence of dansyl-polymyxin was determined repeating the same experiment in the absence of LPS. The decrease in fluorescence due to dansyl polymyxin B displacement was recorded upon addition of 5 µL aliquots of each peptide into a 1 mL cuvette containing 3 µg/mL of LPS and 2.9 µM dansyl-polymyxin (corresponding to 85-90 % of LPS saturation). The data was plotted as percent inhibition *versus* the concentration of peptide (µM), and IC₅₀ values were obtained from these plots. IC₅₀ is defined as the concentration of displacer at which the maximum fluorescence intensity of dansyl-polymyxin/LPS saturated complex is reduced to 50% of the initial value, and was determined by fitting the fluorescence data to a sigmoidal dose-response model assuming a single class of binding sites with GraphPad Prism V5.0 software (GraphPad software, San Diego, CA, USA).

2.6. Kinetics of insertion into monolayers.

Monitoring the insertion of peptides into lipid monolayers at constant area, is a sensitive tool for studying lipid/peptide interactions [21]. Insertion experiments were conducted at 24°C on a KSV5000 system (Helsinki). To avoid carryover of lipid and peptides, the polytetrafluoroethylene (PTFE, Teflon®) trough and the Wilhelmy platinum plate were thoroughly cleaned with double-distilled water at >75 °C. Kinetics of insertion at constant area were monitored as an increase in the surface pressure by use of a cylindrical

trough (5 cm diameter or 19.6 cm² area) containing stirred aqueous phase (30 mL) with 10 mM Tris at pH 8.0. The peptide was added without disturbance of the monolayer via an inlet port in the trough, and the surface pressure was continuously recorded.

2.7. Fluorescence assay for lipid mixing.

Peptide-induced exchange of lipids between vesicles was assessed as described previously [11]. Briefly, transfer of pyrene-labeled phospholipids as donor vesicles (0.83 μ M) to an excess of unlabeled phospholipid vesicles (106 μ M) as acceptors was measured. Emission from vesicles containing 30% pyrene-phospholipid is dominated by the excimer band at 480 nm, and the intensity of the monomer band, at 395 nm, increases as the probe is diluted due to exchange with excess unlabeled vesicles in contact. Experiments were carried out at 24^oC in 10 mM Tris buffer at pH 8.0 on a PTI QM4 spectrophotometer with constant stirring. Peptide was added from a stock solution 0.25 mM in water to the cuvette containing vesicles of the desired composition. Fluorescence emission was monitored at 395 nm (with excitation at 346 nm) corresponding to the monomer emission.

2.8. Leakage of aqueous contents.

Dequenching of coencapsulated ANTS and DPX fluorescence resulting from dilution was measured to assess leakage of aqueous contents. Fluorescence measurements were performed at 24^oC in 10 mM Tris buffer at pH 8.0 on a PTI QM4 spectrophotometer with constant stirring by setting the ANTS emission at 530 nm and the excitation at 350 nm. Peptide was added from a stock solution 0.25 mM in water to the cuvette containing vesicles (lipid concentration 115 μ M). The 0% leakage corresponded to the fluorescence of the vesicle at time zero while 100% leakage was the fluorescence value obtained after addition of Triton X-100 (10% v/v).

2.9. Tryptophan fluorescence

Tryptophan fluorescence spectra were recorded with an excitation wavelength of 285 nm over an emission range 300-450 nm, with 4 nm slit widths. Vesicles were added to a 3 μ M solution of the peptide. Titration of the peptide with vesicles was avoided due to the disruption of the vesicles (fusion and leakage) that occurs at high peptide-to-lipid ratios. The contribution from scattering due to vesicles was subtracted using the same concentration of peptide analogues without tryptophan that induced the same changes in light scattering (control experiments, not shown). In some cases, samples were titrated with NaCl to a final concentration of 350 mM, to determine the influence of increasing ionic strength.

Quenching of tryptophan fluorescence by acrylamide was recorded at 340 nm (excitation 285 nm). Appropriate amounts of POPG, POPE/POPG (6:4) or POPC vesicles, were added to a solution of 3 μ M peptide, and aliquots of quencher were added with continuous stirring. Acrylamide was added from a 4 M stock solution to a final quencher concentration of 0.3 M. The Stern-Volmer quenching constants were evaluated by curve fitting using the following modified equation [22]:

$$\frac{F_0}{F e^{V[Q]}} = 1 + K_{SV}[Q]$$

where F_0 and F are the fluorescence intensities in the absence and presence of the quencher, $[Q]$ is the molar concentration of quencher and V and K_{SV} are the static and dynamic quenching constants.

Steady-state tryptophan fluorescence anisotropy measurements were carried out at 24 $^{\circ}$ C in the same spectrofluorimeter with L-format polarizers (excitation 285 nm, emission 340 nm). Each measure was done in duplicate, independently (no sequential addition of lipid in the same cuvette), adding the vesicles to the desired final lipid concentration to a cuvette containing 3 μ M lipopeptide. The fluorescence anisotropy (r) was calculated according to:

$$r = \frac{I_{Vv} - G I_{Vh}}{I_{Vv} + 2 G I_{Vh}}$$

where I_{Vv} and I_{Vh} are the intensities of the emitted polarizer light with the emission polarizer parallel or perpendicular to the excitation polarizer. Anisotropy values were automatically corrected for dependencies in the detection system ($G=I_{Hv}/I_{Hh}$).

2.10. Fluorescence resonance energy transfer (FRET) to determine peptide binding.

Binding of lipopeptides to vesicles of different composition containing 2.5% of NBD-PE was determined as the increase in the FRET signal from Trp in the peptide to the labeled phospholipid in the interface at 535 nm (excitation 285 nm). Vesicles (33.3 μ M lipid) were titrated with peptide from a stock solution 0.25 mM in water, and the relative change in fluorescence (δF) was obtained. δF is defined as $(F-F_0)/F_0$, where F_0 and F are the intensities without and with peptide, respectively. Due to the low lipid concentration used in this experiment, the contribution from light scattering is negligible.

2.11. Flow cytometry

Bacteria, growth conditions and antimicrobial treatment: An overnight culture (12 to 16 h) of *S. aureus* (ATCC 29213) or *E. coli* (ATCC 25922) in TSB was grown at 37 $^{\circ}$ C and 400 μ L were added in 50 mL of tryptone water ($\sim 10^7$ bacteria/mL). The bacterial suspension was split into aliquots of 4-5 mL and treated with the peptides (at the MIC) for different contact times at room temperature. Cells were collected by

centrifugation (10000 rpm, 20 min) and resuspended in 1 mL of filtered Ringer's solution. *Staining procedure:* A stock solution of PI (1 mg/mL) and BOX (250 μ M) was prepared in distilled water. Portions (10 μ L and 2 μ L, respectively) were added to aliquots of cells (100 μ L of each sample in 1 mL of Ringer's solution) to give a final concentration of 10 μ g.mL⁻¹ (PI) and 0.5 μ M (BOX). Measurements were performed on a Gallios cytometer (Beckman Coulter, CA) set up with the 3-lasers 10 colors standard configuration. Excitation was done using a blue (488 nm) laser. Forward scatter (FS), side scatter (SS), green fluorescence (525/40 nm) from BOX and red fluorescence (620/30 nm) emitted by PI were collected using logarithmic scales. FS was used as the discriminating parameter. The single-cell bacterial population was selected on a forward-side scatter scattergram. Fluorescence was presented in a dot plot of BOX vs. PI. Three regions were defined on this graph according to the controls: depolarized, permeabilized and non-affected cells. Control cells (non-stained and single stained populations) were used to define these regions. 25,000 cells defined according to their scatter parameters were counted in each sample.

3. Results

3.1. Antimicrobial activities of the lipopeptides

Minimal inhibitory concentrations were determined on a Gram negative (*Escherichia coli*) and a Gram positive (*Staphylococcus aureus*) bacteria. As shown in Table 1, all three lipopeptides were active against both types of bacteria, with MIC values in the range from 2.8 to 5.8 μ M. As expected, natural PxB was very effective against *E. coli*, but displayed no antimicrobial activity against *S. aureus*.

Table 1. Peptide sequences used in this work and antibiotic activity in a Gram negative (*Escherichia coli*) and a Gram positive (*Staphylococcus aureus*) bacteria.

	Sequence	MIC μ g.ml ⁻¹ (μ M)	
		<i>E. coli</i>	<i>S. aureus</i>
PxB	R ₁ -Dab-Thr-Dab-cyclo[Dab-Dab-(D)Phe-Leu-Dab-Dab-Thr]	1.0 (0.8)	>128 (102)
sp-34	C ₉ -Arg-Thr-Dab-cyclo-[Cys-Dab-(D)Trp-Leu-Arg-Dab-Cys]	4 (2.9)	8 (5.8)
sp-96	C ₁₀ -Dab-Thr-Arg-cyclo-[Cys-Dab-(D)Trp-Leu-Arg-Dab-(D)Cys]	8 (5.8)	8 (5.8)
sp-100	C ₁₀ -Arg-Thr-Arg-cyclo-[Cys-Dab-(D)Trp-NLeu-Arg-Dab-(D)Cys]	8 (5.5)	4 (2.8)

R₁, (S)-6-methyloctanoyl ; C₉, nonanoyl; C₁₀, decanoyl

3.2. Peptide binding to LPS

Antimicrobial peptides with activity against Gram negative bacteria must first bind to LPS in the outer membrane in order to reach the target inner membrane, a mechanism known as self-promoted uptake [23]. The interaction of the synthetic lipopeptides with LPS from *S. minnesota* was quantified using the dansyl-polymyxin displacement assay. Table 2 shows the maximum displacement relative to non dansylated PxB,

which is taken as 100%, and the peptide concentration needed for 50% of the maximum displacement. IC₅₀ for PxB was 3.6 μM , in agreement with previously reported values [24]. The three lipopeptides show a high affinity for LPS, with maximum displacement of dansyl-polymyxin comparable to that of PxB. The IC₅₀ are even lower than for PxB, with only 2.8 μM in the case of sp-100.

Lipid monolayers of LPS are a good model to study the interaction of the lipopeptides, since LPS forms only the outer layer of the bacterial OM. Insertion of the antibiotic peptides in the LPS monolayer at the air/water interface packed at 32 $\text{mN}\cdot\text{m}^{-1}$ is monitored as an increase in surface pressure vs. time. Results in table 2 correspond to the increases in surface pressure 60 minutes after peptide injection, and clearly sp-34 is the analogue with a higher degree of insertion, with 9 $\text{mN}\cdot\text{m}^{-1}$ of pressure increase, followed by PxB with 5 $\text{mN}\cdot\text{m}^{-1}$. The two analogues with a C10 tail at the N-terminus induced small (around 2 $\text{mN}\cdot\text{m}^{-1}$), but significative increases in surface pressure.

Table 2. Displacement of dansyl-polymyxin bound to LPS from *S. minnesota* by the synthetic analogues

Peptide	I_{max} (%) ^a	IC ₅₀ ^b (μM)	$\Delta\pi^c$ ($\text{mN}\cdot\text{m}^{-1}$)
PxB	100	3.6	5
sp-34	97.4	3.3	9
sp-96	80.9	3.3	2
sp-100	92.5	2.8	2

^amaximum dansyl-polymyxin displacement compared to PxB, taken as 100%; ^bpeptide concentration required for 50% LPS binding; ^cincrease in surface pressure 60 minutes after injection under a monolayer of LPS at 32 $\text{mN}\cdot\text{m}^{-1}$.

3.3. Permeabilization of the lipid membrane induced by the lipopeptides

As shown in Figure 1, the three lipopeptides induced leakage from anionic vesicles, with efficiencies depending on liposome composition. Analogue sp-100 induces permeabilization of POPG liposomes from very low peptide/lipid mole ratios (Fig. 1 *top*). Leakage is very fast upon addition of the peptide, and reaches a constant value until a second aliquot is added, thus suggesting that the peptide is irreversibly bound and an all-or-nothing type of permeabilization. In contrast, lipopeptides sp-34 and sp-96 do not induce significant leakage at peptide/lipid ratios below 0.02:1, very similar to PxB behavior. Increasing the peptide concentration results in leakage but always lower than for the same concentration of sp-100. All three lipopeptides are very effective in inducing leakage from mixed POPE/POPG (6:4) liposomes (Fig. 1 *middle*), with an almost linear increase in permeability at peptide-to-lipid ratios above 0.03, which corresponds to MIC peptide concentration at the onset of antibacterial activity (3 μM), whereas PxB induces almost no leakage at concentrations corresponding to its MIC. Leakage from POPC vesicles is very low in all cases,

although there is some detectable permeabilizing effect that tends to saturate at low peptide/lipid mole ratio (Fig. 1, *bottom panel*).

3.4. Lipid mixing between vesicles due to antimicrobial lipopeptides

As summarized in Figure 2, PxB and the synthetic lipopeptides show selectivity for anionic vesicles, inducing fast exchange of pyr-PG in a concentration-dependent manner, whereas none of the peptides induced significant lipid mixing from zwitterionic POPC vesicles, even at high peptide concentrations. In good agreement with the leakage of contents, the extent of lipid mixing for the same peptide concentration is significantly higher in mixed POPE/POPG (6:4) vesicles, a lipid composition that is more representative of the Gram negative bacterial membranes, than in POPG vesicles. Analogue sp-100 is the most effective lipopeptide in inducing mixing of POPG, followed by sp-34 and sp-96.

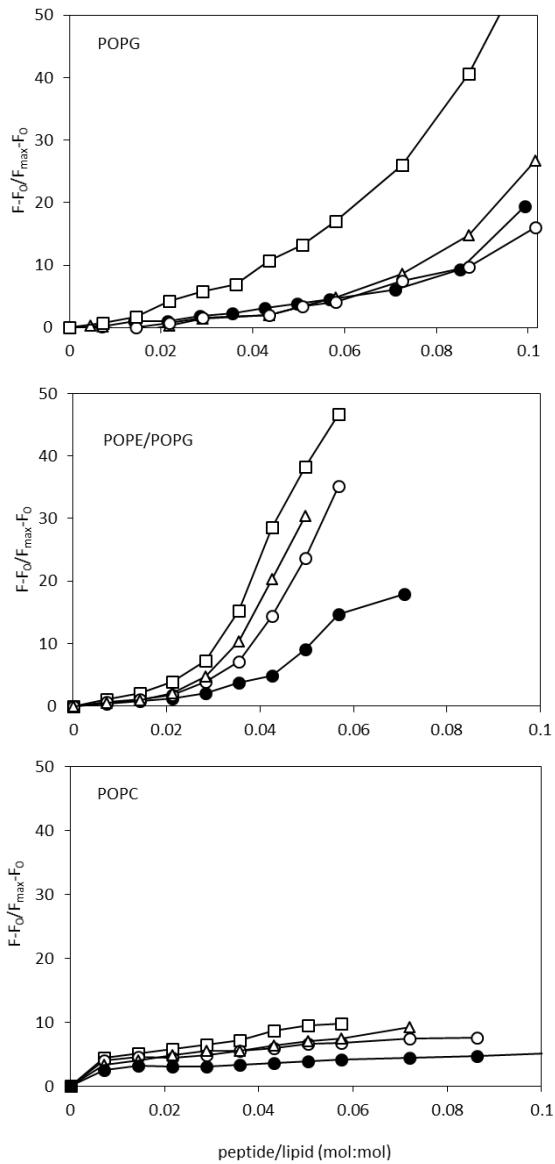


Figure 1. Peptide induced leakage from liposomes of POPG (top), POPE/POPG (6:4) (middle) and POPC (bottom). Increasing concentrations of lipopeptide (\square) sp-100, (\circ) sp-98, (Δ) sp-34 or (\bullet) PxB were added to a solution of liposomes (115 μ M) co-encapsulating ANTS (12.5 mM) and DPX (45 mM), and leakage was monitored as the increase in fluorescence intensity due to ANTS. Excitation 350 nm, emission 530 nm.

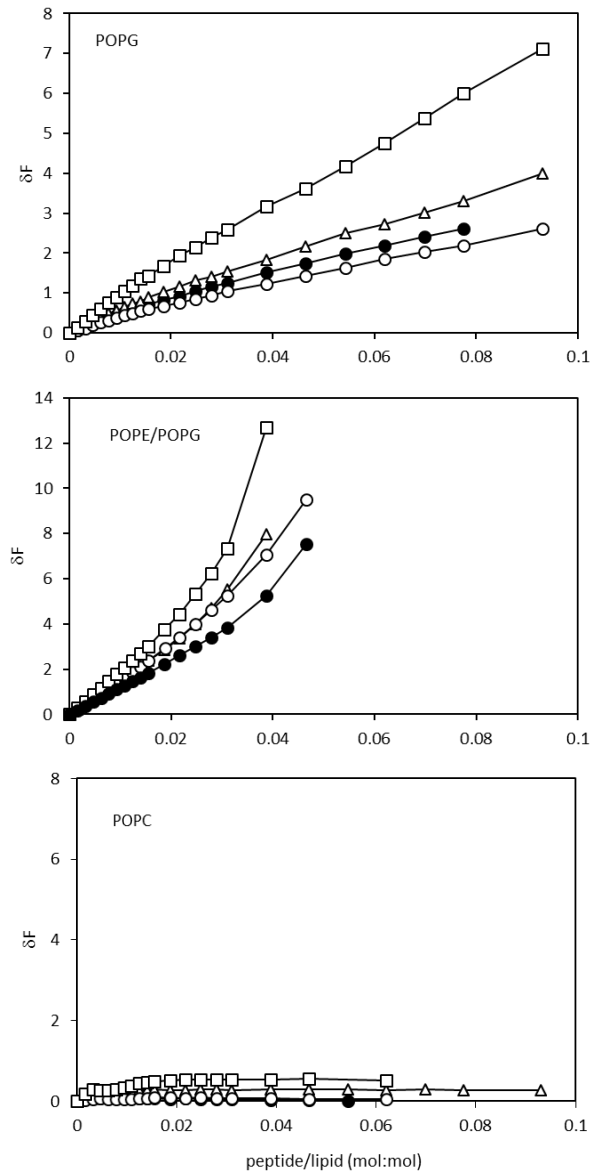


Figure 2. Membrane lipid-mixing induced by the peptides. Increase in fluorescence intensity of pyrene monomer as a function of lipopeptide added to vesicles of different composition. (\square) sp-100, (\circ) sp-98, (Δ) sp-34 or (\bullet) PxB. Vesicles are a mixture of POPG/pyPG, or POPE/pyPG, or POPC/pyPC (0.83 μ M) and unlabeled vesicles of the same composition (106 μ M) in 10 mM Tris pH 8.0. Excitation 346 nm, emission 395 nm. Note the different scales.

3.5. Spectral signatures of the lipopeptides upon binding to the membrane

The emission spectra of all three lipopeptides in buffer has a maximum at 350 nm, indicating that the Trp residue is highly exposed to the solvent (Fig. 3). The fluorescence signatures are markedly altered upon binding to the membrane (Table 3). The first important observation is that sp-34, sp-96 and sp-100 are able to bind not only the anionic vesicles (POPG and POPE/POPG) but the zwitterionic (POPC) too. However, there are important differences depending on the lipid composition, thus reflecting different environments for Trp [25] (Fig. 3). Binding to anionic vesicles of POPG or POPE/POPG results in a blue shift of 15-16 nm of the emission maximum, indicative that the Trp residue is located in a more hydrophobic environment. The blue shift is the same for the three lipopeptides and independent of the peptide-to-lipid ratio. In contrast, differences are seen in the emission intensity, with an important increase in the case of sp-100 bound to POPG, whereas less significant increases are seen on binding of sp-34 and sp-96. The spectral changes for the three lipopeptides in the presence of POPC vesicles are summarized in Table 3; in all cases they show a gradual blue shift on the emission maximum that depends on the lipid concentration. At very low peptide-to-lipid ratio (0.005), when all the peptide is bound, there is a blue shift of 13, 12 and 11 nm for sp-34, sp-96 and sp-100 respectively, accompanied by an increase in the intensity of emission. Increasing the P/L ratio results in smaller blue shift displacements and less significant changes in fluorescence intensity, probably due to an equilibrium between free and bound peptide forms, as also suggested by the presence of an isosbestic point (Fig. 3, *bottom*). Increasing the ionic strength by titrating the samples with NaCl (up to 350 mM) resulted in no backshift of the emission maximum (results not shown), thus indicating that binding was not reversible.

We next determined the changes in anisotropy of tryptophan fluorescence upon binding (Figure 4 and Table 3). Anisotropy values of the free lipopeptides are very low, as expected from a free peptide of this size in solution, where Trp residue has a very high rotational freedom. Binding to POPG vesicles results in an important increase in anisotropy, a clear indication that tryptophan is in a more restricted region due to intercalation of the lipopeptides between the phospholipids. The increase in anisotropy is almost complete at a peptide-to-lipid ratio below 0.01, thus suggesting that all the peptide is bound even at low lipid concentrations. In the case of mixed POPE/POPG vesicles, results are very similar, with slightly lower values of anisotropy compared to pure POPG vesicles. In the case of POPC binding is more gradual, indicating lower affinity, although anisotropy values at high lipid concentration, when all the peptide is bound, are in the same range than in anionic vesicles, for example for sp-100, $r = 0.158$ (in POPG) and 0.150 (in POPC) at the same peptide concentration (Table 3).

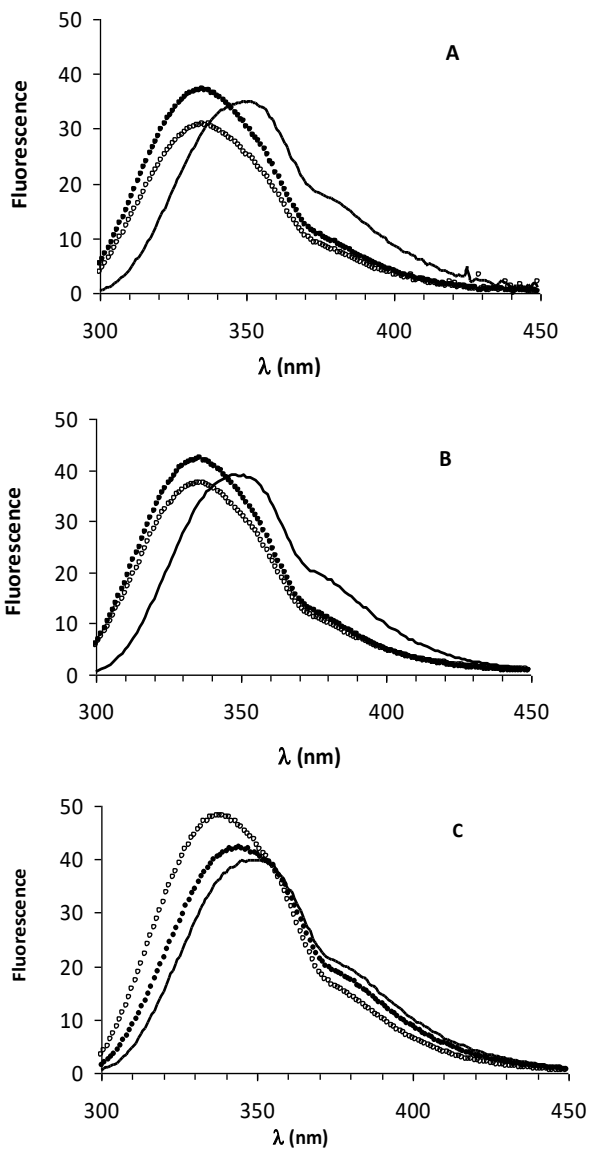


Figure 3. Tryptophan emission spectrum of sp-34 in 10 mM Tris (pH 8.0) (solid line) and in the presence of liposomes composed of POPG (*panel A*), POPE/POPG (6:4 molar ratio) (*panel B*), or POPC (*panel C*). Peptide/lipid molar ratio 0.02 (closed symbols) or 0.005 (open symbols). Peptide concentration was 3 μ M. Excitation 285 nm.

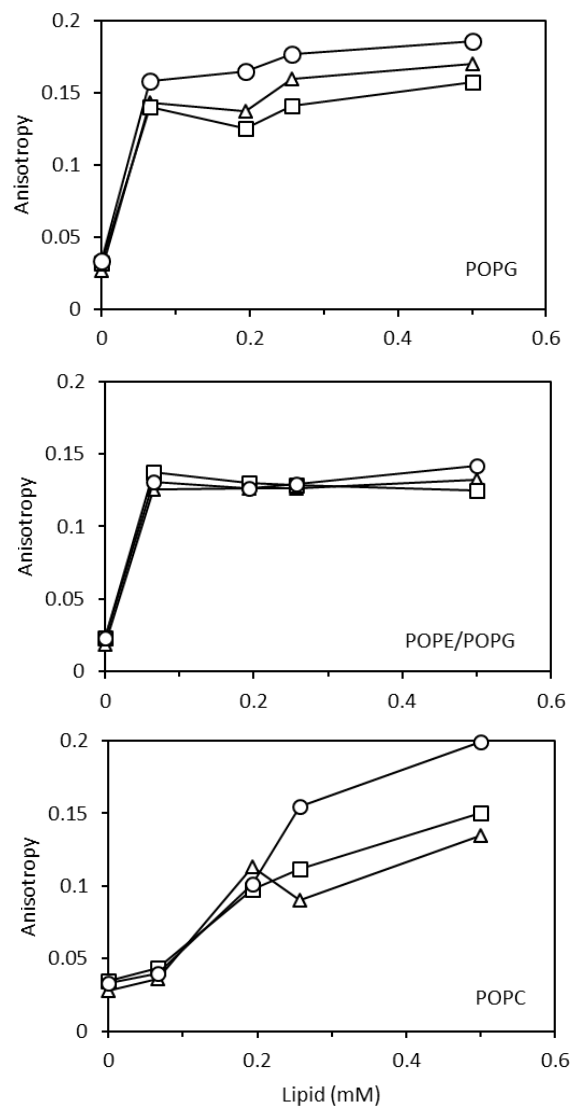


Figure 4. Fluorescence anisotropy change of antibiotic peptides as a function of lipid concentration. (Δ) sp-34, (O) sp-96, (\square) sp-100. Excitation 285 nm, emission 340 nm. Titrations were carried out at 25°C, adding the lipid vesicles to a solution 3 μ M of the desired peptide in 10 mM Tris pH 8.0. Each point corresponds to a separate experiment.

Table 3. Tryptophan fluorescence properties of peptides sp-34, sp-96 and sp-100 in the presence of liposomes of POPG, POPE/POPG (6:4) and POPC at two different peptide/lipid molar ratios (0.02 and 0.005)

Conditions	λ_{\max} (nm)			F/F_0^a			Anisotropy (r)		
	sp-34	sp-96	sp-100	sp-34	sp-96	sp-100	sp-34	sp-96	sp-100
free peptide	350	350	350	--	--	--	0.028	0.033	0.033
POPG, P/L = 0.02	335	335	336	1.07	1.15	1.64	0.137	0.165	0.126
POPG, P/L = 0.005	336	336	337	0.89	0.96	1.45	0.170	0.185	0.158
POPE/POPG, P/L = 0.02	336	335	335	1.09	1.19	1.06	0.126	0.126	0.130
POPE/POPG, P/L = 0.005	337	337	336	0.96	1.07	0.96	0.132	0.142	0.128
POPC, P/L = 0.02	344	343	345	1.06	1.08	1.05	0.114	0.102	0.100
POPC, P/L = 0.005	337	338	339	1.21	1.23	1.34	0.135	0.200	0.150

(a) F is the peptide fluorescence intensity in the presence of liposomes at the wavelength of maximum emission, and F_0 is the fluorescence of the free peptide at 350 nm.

3.6. Quenching of (D)Trp by acrylamide

Results described in the previous section indicate that for sp-34, sp-96 and sp-100, (D)Trp⁷ intercalates into the hydrophobic core of the membrane. We next investigated to what extent this residue is exposed to the aqueous phase, by using the water-soluble quencher of indole derivatives acrylamide (Table 4). Free lipopeptides show very high quenching constants, both dynamic and static, indicating that (D)Trp is highly accessible to acrylamide. K_{SV} and V values for sp-100, sp-96 and sp-34 are very similar, around 12 M⁻¹ and 3 M⁻¹ respectively. When the lipopeptides were bound to POPG, quenching became less efficient, for example for sp-34 at P/L = 0.005, K_{SV} and V values were 3.439 M⁻¹ and 1.330 M⁻¹, and very similar quenching constants were obtained for sp-96 and sp-100. In agreement with anisotropy results (Fig. 4), Trp-accessibility was independent of the peptide-to-lipid ratio. Results obtained with mixed POPE/POPG are also consistent with a high degree of shielding of the Trp residue from the aqueous solvent due to insertion in the bilayer, without significant differences with the insertion into POPG vesicles. Finally, for POPC at P/L of 0.02, the higher value of the K_{SV} constant, for example 7.545 M⁻¹ for sp-34 and around 10 M⁻¹ for sp-96 and sp-100, is indicative of a more exposed tryptophan, or more likely to an equilibrium between free and bound peptide. Increasing the lipid concentration (P/L 0.005) favors peptide binding, with lower values of the collisional quenching constant.

Table 4. Acrylamide quenching constants (M^{-1}) for antibacterial peptides sp-34, sp-96 and sp-100. K_{SV} and V are the dynamic and static quenching constants respectively.

Conditions		sp-34	sp-96	sp-100
10 mM Tris pH 8.0	K_{SV}	12,4	12,46	11,99
	V	2,867	2,878	3,04
POPG, P/L = 0.02	K_{SV}	3,317	2,769	3,101
	V	1,396	1,719	1,524
POPG, P/L = 0.005	K_{SV}	3,439	3,621	3,298
	V	1,338	1,335	1,477
POPE/POPG, P/L = 0.02	K_{SV}	3.245	2.486	3.428
	V	1.283	1.483	1.152
POPE/POPG, P/L = 0.005	K_{SV}	3.673	2.209	3.591
	V	1.073	1.283	1.049
POPC, P/L = 0.02	K_{SV}	7,545	10,3	10,02
	V	0,7895	0,8885	0,4384
POPC, P/L = 0.005	K_{SV}	3,535	6,939	5,69
	V	1,51	1,113	1,237
Quenching constants were obtained by fitting of data according to ref. 22, with r^2 values always above 0,9998. Peptide concentration 3 μM ; acrylamide range 0-350 mM.				

3.7. Binding of lipopeptides to vesicles determined by FRET

The different results in Trp emission fluorescence of sp-34, sp-96 and sp-100 bound to POPG vs. POPC vesicles can be due to lower peptide binding to the zwitterionic vesicles or to a different form of the bound peptide. In order to distinguish these two possibilities, binding of all three lipopeptides to vesicles containing NBD-PE was determined. As shown in Figure 5, FRET intensity increases with the amount of peptide added. In the anionic POPG vesicles (Fig. 5 top) FRET signal did not saturate even at very high peptide-to-lipid ratios, indicating a very efficient binding. The presence of POPE results in higher FRET for the same peptide-to-lipid ratio. For example, in sp-34 at P/L=0.05, the relative increase in fluorescence (δF) is 4.96 for the POPE containing vesicles and 3.74 for pure POPG vesicles. The synthetic antimicrobial peptides also show binding to POPC vesicles, with a small FRET signal that in this system saturates at P/L around 0.02 (Fig. 5 bottom). When POPG-labeled vesicles were added to a premixed sample containing any of the lipopeptides with POPC vesicles, the FRET signal obtained was much lower than the one under the same conditions but without POPC (not shown). For example, for sp-100 binding to POPG vesicles (33.3 μM) at P/L 0.02, δF is 1.6, but if the POPG vesicles are added to a mixture of POPC (33.3 μM) with sp-100 (0.66

μM), a much lower FRET signal is obtained (δF is 0.32), indicating that the lipopeptide is effectively bound to POPC.

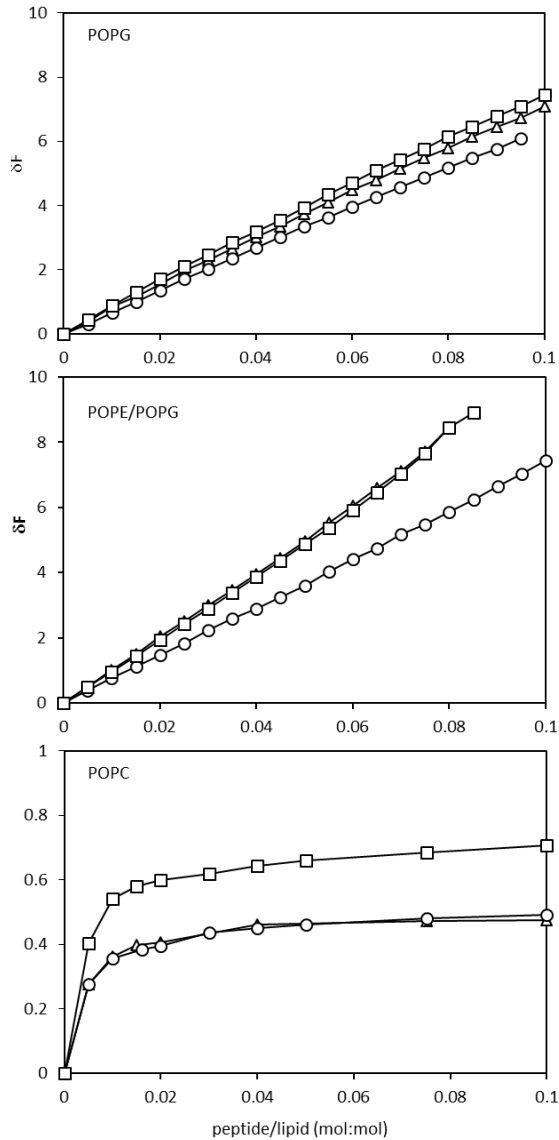


Figure 5. Change in FRET intensity at 535 nm (excitation at 285 nm) resulting from the addition of lipopeptides to vesicles containing 2.5% NBD-PE. (\square) sp-100, (\circ) sp-96, (Δ) sp-34. Lipid concentration 33 μM .

3.8. Effect on the bacterial membrane potential and integrity by flow cytometry

Peptide sp-100 was chosen for FC analysis due to the results obtained with the biophysical experiments where it demonstrated high membrane activity. To assess the affectation of the membrane due to peptide interaction two dyes were used, a DNA-labelling dye (PI) and a potential-sensitive dye (BOX). PI is a non-permeable fluorochrome that intercalates into double-stranded nucleic acid and is excluded by viable cells,

therefore measurement of the loss of viability produced by antimicrobial agents or other compounds is possible [26]. BOX accumulates inside the bacterial cell depending on the difference in charge between the two sides of the plasma membrane and therefore differences in membrane potential, due to peptide interaction, can be measured [27]. As reported in Figure 6, in *E. coli* cells treated with sp-100 at the MIC of 8 µg/ml, a gradual uptake of PI can be observed together with a reduction of viability determined by parallel cell count, while the cells with dissipation of membrane potential but without permeabilization only reach 20-30 %. In contrast, in *S. aureus* sp-100 causes rapid depolarization, as indicated by BOX fluorescence, but membrane permeabilization is less significant and appears after depolarization. For example, after 30 minutes of exposure there is no significant permeabilization; a maximum value of 20% is reached at 60 minutes and more contact time did not result in a higher PI uptake, while depolarization of the membrane increased gradually with contact time.

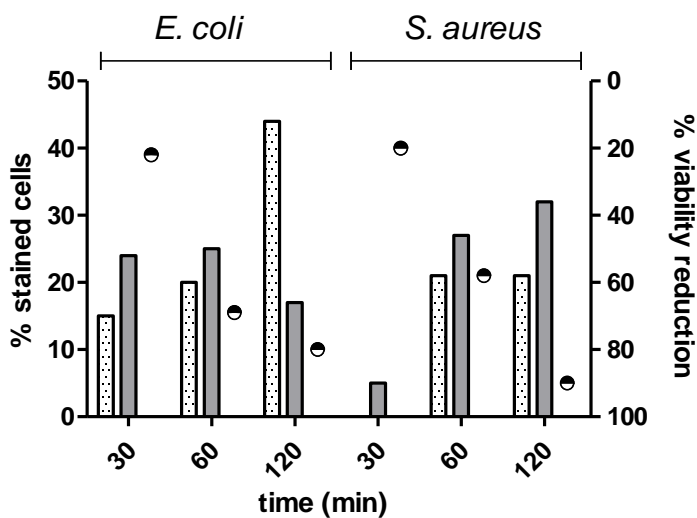


Figure 6. Effect of sp-100 on the bacterial membrane determined by flow cytometry. *E. coli* or *S. aureus* cell samples were incubated with sp-100 at the MIC of 8 µg/ml at the indicated times. Dotted columns show cells stained with PI, corresponding to permeabilized membranes, and grey columns are cells stained with BOX (but not with PI), therefore cells that are depolarized. Viability reduction determined by plate count is plotted as symbols. Controls of untreated cells with the same incubation times (<5%) are already subtracted.

4. Discussion

New antimicrobial lipopeptides derived from PxB have a wide spectrum of activity. Polymyxins, including PxB and colistin, are increasingly being used as last-line therapy to treat infections caused by multiresistant

Gram negative bacteria due to their good antimicrobial activity and relatively low prevalence of resistance [6,8]. In an effort to discover new antimicrobial lipopeptides with a better therapeutic index, we have previously described several analogues based on the structure of natural PxB. The head-compound is sp-B [14]. Sp-B maintains the major putative structural requirements for PxB activity: a cycle of 7 amino acids with 3 positive charges due to L- α,γ -diaminobutyric acid (Dab) and a hydrophobic domain (D)-Phe-Leu, a linear tripeptide with 2 positive charges also due to Dab, and a middle length hydrophobic N-terminal chain. In addition, sp-B includes a disulfide bridge between two cystein residues to simplify the synthetic process. Sp-B interaction with phospholipid vesicles is analogous to the interaction of PxB [14,15]. In this paper, we describe three new lipopeptides (Table 1) based on the scaffold of sp-B and including different key modifications. They are members of a family of more than 100 analogues synthesized and tested so far [16, 28-30], and share a (D)Trp⁷, thus conferring the molecules an intrinsic fluorescence that is very useful to characterize membrane binding. The analogues also contain residues of arginine in positions 1-8 (sp-34), 3-8 (sp-96) and 1-3-8 (sp-100), substituting residues of the non-natural aminoacid Dab. Both Trp and Arg residues are known to possess crucial chemical properties that make them suitable components of antimicrobial peptides [31,32]. Tryptophan favors the interaction with the interfacial region of the lipid membrane, whereas arginine, apart from the cationic charge that is necessary for electrostatic binding to the anionic bacterial phospholipids, has better hydrogen bonding properties than Dab or Lys. Arg can form cation- π interactions that make the entry into the hydrophobic core of the bilayer energetically more favorable. Since most AMPs achieve their bactericidal effect with an initial interaction with the outer and/or inner membranes of bacteria, which often is also the site of action, electrostatic and hydrophobic interactions with the lipid components are pivotal for activity. For example, in the antimicrobial peptide protegrin-1, with two Arg, it has been suggested that guanidinium-phosphate complexation, which neutralizes the guanidinium ions before they are inserted into the membrane, results in toroidal-pore formation [33]. In addition, in sp-96 and sp-100, the C-terminal Cys residue is mutated to a (D)Cys, to better mimic the conformation of the natural residue of Thr¹⁰ in PxB. Finally, a key mutation is the introduction of NLeu instead of Leu in position 7 in sp-100, to increase flexibility in this strategic hydrophobic residue. Lipopeptides sp-34, sp-96 and sp-100 have good antimicrobial activities against *E. coli* and *S. aureus*, in contrast with the selectivity for Gram negative bacteria that characterizes PxB. We have recently reported the *in vitro* cytotoxicity of PxB-analogs of the same family, containing two or three residues of Arg but without Trp [16]. Results obtained on different cell cultures of mammalian cells indicated low toxicity, with IC₅₀ values always above 450 $\mu\text{g}\cdot\text{ml}^{-1}$.

Gram negative bacteria have an outer membrane composed mainly of LPS, and LPS binding is a necessary first step for antimicrobial action. Antibiotic peptides must enter the periplasmic space by self promoted uptake, displacing divalent cations that keep the LPS molecules densely packed, before they reach the inner membrane which is generally considered to be the primary target, or other intracellular targets [23]. We have shown that sp-34, sp-96 and sp-100 have a high affinity for LPS, comparable to that of native PxB, displacing previously bound dansyl-polymyxin from LPS. All lipopeptides insert into LPS monolayers at $32 \text{ mN}\cdot\text{m}^{-1}$, a lateral pressure that is in the order of the biological membrane [34]. The longer N-terminal acyl chain of sp-96 and sp-100 results in lower increases in surface pressure, probably because the peptidic moiety of the bound lipopeptide can accommodate at the interfacial region of LPS. The interaction between polymyxins and the lipid A part of LPS has been well characterized at the molecular level by NMR and molecular modeling techniques [8,35,36]. The backbone of PxB is folded in an envelope-like fold, separating the polar residues from the hydrophobic components, thus conferring the structure an amphipathic character. The hydrophobic residues (D)Phe⁶ and Leu⁷, as well as the N-terminal acyl chain, penetrate into the hydrocarbon portion of LPS, whereas the polar residues are oriented to point into the hydrophilic environment of the OM. The complex is stabilized by electrostatic interactions between the positive charges of the Dab side chains and the phosphates in lipid A. Results obtained with the synthetic peptides point towards a similar interaction with LPS, and we can conclude that they will also destabilize the OM.

Fluorescence spectroscopy shows differential binding to POPG, POPE/POPG and POPC model membranes. We next studied the interaction of the lipopeptides with liposomes that mimic the cytoplasmic membrane of bacteria. Liposomes of pure POPG and mixed POPE/POPG (6:4 mol/mol), were chosen as models, based on the reported membrane composition of different bacterial types [17]. In general, cytoplasmic membranes of Gram positive bacteria are mostly composed of anionic lipids, whereas high contents of PEs are found in Gram negative bacteria. Vesicles of zwitterionic POPC were also prepared as models of the eukaryotic membrane. FRET experiments show that antimicrobial lipopeptides sp-34, sp-96 and sp-100 bind with high affinity to anionic vesicles of POPG and POPE/POPG (6:4), with a linear dependence between FRET intensity and peptide concentration. The higher increase in NBD fluorescence observed in POPE/POPG vesicles indicates that the presence of the zwitterionic POPE favors peptide binding. Although it is generally accepted that cationic antimicrobial peptides interact with bacterial membranes mainly through electrostatic interactions with the anionic phospholipid head groups [37-39], FRET results shown here demonstrate that zwitterionic POPE also plays an important role. Tryptophan fluorescence emission spectra, anisotropy measurements and quenching experiments were conducted to

characterize the membrane bound form of the three lipopeptides. All three showed comparable fluorescence characteristics in buffer, with the fluorescence maxima centered at 350 nm, indicative of Trp residues located in a hydrophilic environment [40]. In addition, similar emission intensities reveal a similar environment for tryptophan. The very low Trp-anisotropy values and high Trp-quenching constants are consistent with the absence of a folded structure in solution. In the presence of the anionic membranes, modifications in Trp fluorescence properties are a clear indication of binding and insertion into a more hydrophobic environment. The observed blue-shift of around 15 nm, and the significant increases in anisotropy are relatively independent on lipid concentration, and indicate that Trp is in a more hydrophobic region of the bilayer, where it remains relatively immobilized. Acrylamide quenching is consistent with low accessibility to the aqueous phase. We can conclude that sp-34, sp-96 and sp-100 bind more efficiently to POPE-containing POPG vesicles than to pure POPG vesicles, but the three peptides bind in similar forms with equivalent spectroscopic properties. Binding to POPC vesicles is significantly less efficient, with a lower intensity in the FRET signal that saturates at peptide-to-lipid ratios above 0.02. Spectral signatures in POPC vesicles are consistent with a more gradual, concentration-dependent insertion of the lipopeptide. The absence of salt effect is indicative of an irreversible binding to the membrane, consistent with the deep insertion of the three lipopeptides. Similar results were obtained for the pore-forming cyclic antimicrobial peptide BPC194 on binding to anionic membranes [41].

Peptide-induced perturbation of the membrane requires the presence of anionic lipids. Leakage experiments show that the three lipopeptides are able to permeabilize vesicles of POPE/POPG in a concentration-dependent manner. Sp-100 is the more lytic lipopeptide in this model system, and shows a biphasic pattern, with higher membrane-permeabilizing effect above $P/L = 0.03$, which corresponds to $4 \mu\text{M}$ peptide (the MIC for this lipopeptide against *E. coli* is $5.5 \mu\text{M}$). This elevated peptide-to-lipid ratio suggests that possibly sp-100 acts by the “carpet” mechanism, where a minimum amount of bound peptide is needed before channels are formed [42]. Lipopeptides sp-34 and sp-96 are only slightly less permeabilizing at the same P/L ratio. In contrast, natural PxB has no permeabilizing effect at concentrations corresponding to its MIC for *E. coli*. All three synthetic lipopeptides induce mixing of phospholipids between vesicles of POPE/POPG. The efficacy of causing lipid mixing follows the same trend as the ability to induce leakage, with sp-100 being the most active peptide. Therefore, sp-100, sp-34 and sp-96 cause leaky fusion of POPE/POPG vesicles at concentrations relevant to their antimicrobial activity in *E. coli*, thus suggesting a mechanism of action based on the permeabilization of the cytoplasmic membrane. The possibility of an unspecific detergent effect with formation of micelles can be ruled out as demonstrated by a peptide concentration-dependent increase in light scattering of the anionic vesicles, indicative of an increase in

particle size by clustering of the vesicles (results not shown), as is also the case with PxB and sp-B [14], and with sp-85, an analogue of PxB that shows broad spectrum of activity [43]. Interaction of sp-85 with lipid monolayers at the membrane equivalence pressure results in an alteration on lipid packing that is consistent with membrane fusion and leakage induced upon binding to liposomes of the same composition, and further confirmed by TEM images of treated bacteria, with significant modifications on the bacterial cell membrane. This behavior is common to other antimicrobial peptides, such as MSI-78 and LL-37 [44,45], and can be related to the negative spontaneous curvature imparted by POPE, due to the fact that the polar headgroup has a smaller diameter than the hydrocarbon chain region in the fluid phase, and the increased acyl chain packing induced by this lipid [46,47]. Many AMPs are known to induce clustering of anionic lipids, causing lipid segregation and, as a result, leakage of aqueous contents and/or membrane depolarization [5,47]. The biological significance of membrane fusion is poorly understood, however it is likely that the process enables the translocation of the peptide molecules across the membrane bilayer [48]. In contrast, results with PxB are consistent with a different mechanism of action based on the mixing of lipids between the outer and inner membranes and the resulting osmotic imbalance [12,49]. In POPG vesicles differences among the lipopeptides are more important, with a weaker effect of sp-34 and sp-96 on the permeability of the membrane compared to a fast leakage of aqueous contents induced by sp-100. Also, the efficacy of causing lipid mixing follows the same trend as the ability to induce leakage. The effects of sp-34 and sp-96 in this system are closer to PxB than to sp-100, which is surprising considering the different MIC values ($>102 \mu\text{M}$ for PxB and $5.8 \mu\text{M}$ for the analogues). There are other examples of antimicrobial peptides that cause no significant leakage or fusion in model membranes at concentrations corresponding to their MIC and above. In fact, although the mode of action of many AMPs involves disruption of the bacterial membrane integrity, other antimicrobial mechanisms have recently been characterized that target key cellular processes such as DNA and protein synthesis, protein folding, enzymatic activity and cell wall synthesis [5]. Some AMPs can even have several targets, a multi-hit strategy that increases their efficiency reducing the possibility of resistance [50]. For example, the Ca^{+2} -dependent antibiotic lipopeptide MX-2401, an analogue of amphomycin, inhibits peptidoglycan synthesis by binding to the substrate undecaprenylphosphate, without affecting membrane integrity [51]. It is also possible that sp-34 and sp-96 kill the bacteria by inducing non-lytic depolarization, thus dissipating the membrane potential without further damage. This mechanism has been described for daptomycin [51], lactoferricin [52] and certain ceragenins [53]. Even though the synthetic lipopeptides bind to zwitterionic POPC membranes, they do not induce significant leakage or fusion, thus suggesting that they may not be toxic in eukaryotic cells. These results also emphasize the importance of choosing the membrane composition to obtain relevant results: although cationic peptide antimicrobial

peptides interact with bacterial membranes mainly through electrostatic interactions with the POPG head groups, this cannot be the only governing factor, because the nature of the additional lipid components also play a role, as demonstrated with aurein 2.2 and derivatives [54] and plantaricin A [55].

Flow cytometry results are consistent with a membrane-based mechanism of action for sp-100 in both *E. coli* and *S. aureus*. Time-response assays show that in *S. aureus* collapse of membrane potential occurs before collapse of membrane integrity, whereas in *E. coli* depolarization and permeabilization take place roughly at the same time, and PI fluorescence increases with the time of incubation. Viability reduction obtained by plate count is generally in good correlation with membrane damage caused by the peptide. For example, in *S. aureus* after 60 minutes of incubation with sp-100, 22% of cells are permeabilized (PI-stained), and 32% are only depolarized (BOB-stained), therefore a total of 54% of cells are damaged, which is consistent with the observed 58% of cell death. FC data is in good agreement with the biophysical experiments in model membranes, with more permeabilization from *E. coli* than from *S. aureus*, corresponding to more leakage from POPE/POPG vesicles than for pure anionic POPG vesicles at the same peptide concentration.

5. Conclusions

We report three new synthetic antimicrobial lipopeptides with Gram positive and Gram negative activity derived from the structure of the Gram negative selective antibiotic PxB. Biophysical studies with model membranes show that the peptides bind to zwitterionic and anionic membranes, but they require the presence of anionic lipids to disrupt the membrane. The inclusion of Arg residues instead of natural Dab favors the insertion in the bacterial lipid membrane and allows passage of the peptides across the bilayer. The presence of (D)Trp favors membrane interaction and confers the molecule intrinsic fluorescence properties that allow the determination of membrane binding. The substitution of Leu by the more flexible NLeu increases the permeabilizing and fusogenic capacity. The new lipopeptides described here are good candidates to become new antimicrobials, although further work needs to be done to ascertain their molecular mechanism of action.

ACKNOWLEDGEMENTS

We thank MICINN (CTQ2008-06200), Generalitat de Catalunya (VAL-TEC 08-1-0016, ACC10), Xarxa de Referència en Biotecnologia and Fundació Bosch i Gimpera (UB) for supporting this work. FR, YC and AM are members of the ENABLE consortium (European Network for Antibiotic Lead Engine, 7th FP and EFPIA, IMI-JU 8th call).

REFERENCES

- [1] Walsh, Ch.T.; Wencewicz, T.A. Prospects for new antibiotics: a molecule-centered perspective. *J. Antibiot.* **2014**, *67*, 7–22.
- [2] Fauci, A.S. Infectious Diseases: Considerations for the 21st Century. *Clin. Infect. Dis.* **2001**, *32*, 675-685.
- [3] Boucher, H.W.; Talbot, G.H.; Bradley, J.S.; Edwards, J.E.; Gilbert, D.; Rice, L.B.; Scheld, M.; Spellberg, B.; Bartlett, J. Bad Bugs, No Drugs: No ESKAPE! An Update from the Infectious Diseases Society of America. *Clin. Infect. Dis.* **2009**, *48*, 1-12.
- [4] Brodgen, K.A. Antimicrobial peptides: pore formers or metabolic inhibitors in bacteria? *Nature* **2005**, *3*, 238-250.
- [5] Nguyen, L.T.; Haney, E.F.; Vogel, H.J. The expanding scope of antimicrobial peptide structures and their modes of action. *Trends Biotechnol.* **2011**, *29*, 464-472.
- [6] Pogue, J.M.; Marchaim, D.; Kaye, D.; Kaye, K. S. Revisiting “older” antimicrobials in the era of multidrug resistance. *Pharmacotherapy* **2011**, *31*, 912-921.
- [7] Yeaman, M.R.; Yount, V. Mechanisms of antimicrobial peptide action and resistance. *Pharmacol. Rev.* **2003**, *55*, 27–55.
- [8] Velkov, T.; Thompson, P.E.; Nation, R.L.; Li, J. Structure–activity relationships of polymyxin antibiotics. *J. Med. Chem.* **2010**, *53*, 1898-1916.
- [9] Talbot, G.H.; Bradley, J.; Edwards, J.E., Jr.; Gilbert, D.; Scheld, M.; Bartlett, J.G. Bad bugs need drugs: an update on the development pipeline from the Antimicrobial Availability Task Force of the Infectious Diseases Society of America. *Clin. Infect. Dis.* **2006**, *42*, 657–668.
- [10] Cajal, Y.; Rogers, J.; Berg, O.G.; Jain, M.K. Intermembrane molecular contacts by polymyxin B mediate exchange of phospholipids. *Biochemistry* **1996**, *35*, 299-308.
- [11] Cajal, Y.; Ghanta, J.; Easwaran, K.; Surolia, A.; Jain, M. K. Specificity for the exchange of phospholipids through polymyxin B mediated intermembrane molecular contacts. *Biochemistry* **1996**, *35*, 5684-5695.
- [12] Oh, J-T.; Van Dyk, T.K.; Cajal, Y.; Dhurjati, P.S.; Sasser, M.; Jain, M.K. Osmotic stress in viable *Escherichia coli* as the basis for the antibiotic response by polymyxin B. *Biochem. Biophys. Res. Comm.* **1998**, *246*, 619-623.
- [13] Oh, J-T ; Cajal, Y.; Skowronska, E.M.; Belkin, S.; Chen, J.; Van Dyk, T.K.; Sasser, M.; Jain, M.K. Cationic peptide antimicrobials induce selective transcription of *micF* and *osmY* in *Escherichia coli*. *BBA-Biomembranes* **2000**, *1463*, 43-54.

- [14] Clausell, A.; Rabanal, F.; Garcia-Subirats, M.; Alsina, M.A.; Cajal, Y. Membrane association and contact formation by a synthetic analogue of polymyxin B and its fluorescent derivatives. *J. Phys. Chem. B* **2006**, *110*, 4465-4471.
- [15] Clausell, A.; Garcia-Subirats, M.; Pujol, M.; Busquets, M. A.; Rabanal, F.; Cajal, Y. Gram negative outer and inner membrane models: Insertion of cyclic cationic lipopeptides. *J. Phys. Chem. B* **2007**, *111*, 551-563.
- [16] Rabanal, F.; Grau-Campistany A.; Vila-Farrés, X.; Gonzalez-Linares, J.; Borràs, M.; Vila, J.; Manresa, M.A; Cajal, Y. New cyclic lipopeptides with high activity against resistant bacteria and low *in vivo* toxicity. *Scientific Reports* **2015**, *5*, 10558.
- [17] Epand R.M., Rotem S., Mor A., Berno, B., Epand, R.F. Bacterial membranes as predictors of antimicrobial potency. *J. Am. Chem. Soc.* **2008**, *130*, 14346-14352.
- [18] Rabanal, F.; Tusell, J. M.; Sastre, L.; Quintero, M. R.; Cruz, M.; Grillo, D.; Pons, M.; Albericio, F.; Serratos, J.; Giralt, E. Structural, kinetic and cytotoxicity aspects of 12–28 β -amyloid protein fragment: a reappraisal. *J. Peptide Sci.* **2002**, *8*, 578–588.
- [19] Woods, G.L.; Washington, J.A. Antibacterial susceptibility test: dilution and disk diffusion methods in: *Manual of Clinical Microbiology*. 6th ed. Murray, O.R. eds. American Society for Microbiology. Washington DC. **1995**, 1327-1341.
- [20] Fidai, S.; Farmer, S.W.; Hancock, R.E. Interaction of cationic peptides with bacterial membranes. In: *Methods in Molecular Biology Vol. 78: Antibacterial peptides protocols*. Shafer W.M. ed. Humana Press Inc. Totowa NJ. **1997**, 187-204.
- [21] Maget-Dana, R. The monolayer technique: a potent tool for studying the interfacial properties of antimicrobial and membrane-lytic peptides and their interactions with lipid membranes. *BBA-Biomembranes* **1999**, *1462*, 109-140.
- [22] Eftink, M.R.; Ghiron, C.A. Fluorescence quenching of indole and model micelle systems. *J. Phys. Chem.* **1976**, *80*, 486-493.
- [23] Hancock, R.E.W. Peptide antibiotics. *Lancet* **1997**, *349*, 418-422.
- [24] Patrzykat, A.; Friedrich, C.L.; Zhang, L.; Mendoza, V.; Hancock, R.E.W. Sublethal concentrations of pleurocidin-derived antimicrobial peptides inhibit macromolecular synthesis in *Escherichia coli*. *Antimicrob. Agents Ch.* **2002**, *46*, 605-614.
- [25] Galla, H.J.; Warncke, M.; Scheit, K.H. Incorporation of the antimicrobial protein seminalplasmin into lipid bilayer membranes. *Eur Biophys J.* **1985**, *12*, 211-216.

- [26] Gant, V.A.; Warnes, G.; Phillips, I.; Savidge, G.F. The application of flow cytometry to the study of bacterial responses to antibiotics. *J. Med. Microbiol.* **1993**, *39*, 147–154.
- [27] Comas, J.; Vives-Rego, J. Assessment of the effects of gramicidin, formaldehyde, and surfactants on *Escherichia coli* by flow cytometry using nucleic acid and membrane potential dyes. *Cytometry* **1997**, *29*, 58–64.
- [28] Rabanal, F.; Cajal, Y.; Garcia-Subirats, M.; Rodríguez, M. Patent ES2008/02626; WO2010/029196 A1.
- [29] Rabanal, F.; Cajal, Y.; García, M.; Rodríguez M. Patent ES201000349, ES 2.374.779 A1, WO 2011 110716, US 2013 053305.
- [30] Rabanal, F.; Cajal, Y.; Grau-Campistany, A.; Vila, J.; Vila, X. Patent P201330519, PCT/ES2014/070286.
- [31] Chan, D. I.; Prenner, E. J.; Vogel, H. J. Tryptophan- and arginine-rich antimicrobial peptides: Structures and mechanisms of action, *BBA-Biomembranes* **2006**, *1758*, 1184–1202.
- [32] Arouri, A.; Dathe, M.; Blume, A. Peptide induced demixing in POPG/POPE lipid mixtures: A mechanism for the specificity of antimicrobial peptides towards bacterial membranes? *BBA-Biomembranes* **2009**, *1788*, 650-659.
- [33] Tang, M.; Waring, A.J.; Hong, M. Phosphate-mediated arginine insertion into lipid membranes and pore formation by a cationic membrane peptide from solid-state NMR. *J. Am. Chem. Soc.* **2007**, *129*, 11438-11446.
- [34] Marsh, D. Lateral pressure in membranes. *BBA-Biomembranes* **1996**, *1286*, 163-223.
- [35] Bruch, M.D.; Cajal, Y.; Koh, J.T.; Jain, M.K. Higher-Order Structure of Polymyxin B: The functional significance of topological flexibility. *J. Am. Chem. Soc.* **1999**, *121*, 11993-12004.
- [36] Pristovsek, P.; Kidric, J. Solution structure of polymyxins B and E and effect of binding to lipopolysaccharide: an NMR and molecular modeling study. *J. Med. Chem.* **1999**, *42*, 4604–4613.
- [37] Dathe, M.; Nikolenko, H.; Meyer, J.; Beyermann, M.; Bienert, M. Optimization of the antimicrobial activity of magainin peptides by modification of charge. *FEBS Lett.* **2001**, *501*, 146–150.
- [38] Papo, N.; Shai, Y. Host defense peptides as new weapons in cancer treatment. *Cell. Mol. Life Sci.* **2005**, *62*, 784–790.
- [39] Matsuzaki, K.; Sugishita, K.; Fujii, N.; Miyajima, K. Molecular basis for membrane selectivity of an antimicrobial peptide, magainin 2. *Biochemistry* **1995**, *34*, 3423–3429.
- [40] Burstein, E. A.; Vedenkina, N. S.; Ivkova, M. N. Fluorescence and the location of tryptophan residues in protein molecules. *Photochem. Photobiol.* **1973**, *18*, 263-279.

- [41] Mika, J.T.; Moiset, G.; Cirac, A.D.; Feliu, L.; Bardají, E.; Planas, M.; Sengupta, D.; Marrink, S.J.; Poolman, B. Structural basis for the enhanced activity of cyclic antimicrobial peptides: The case of BPC194. *BBA-Biomembranes* **2011**, *1808*, 2197–2205.
- [42] Pouny, Y.; Rapaport, D.; Mor, A.; Nicolas, P.; Shai, Y. Interaction of antimicrobial dermaseptin and its fluorescently labeled analogues with phospholipids membranes. *Biochemistry* **1992**, *31*, 12416–12423.
- [43] Grau-Campistany, A.; Pujol, M.; Marqués, A.M.; Manresa, A.; Rabanal, F.; Cajal, Y. Membrane interaction of a new synthetic antimicrobial lipopeptide sp-85 with broad spectrum activity. *Colloids Surf. A: Physicochem. Eng. Aspects* **2015**, *480*, 307-317.
- [44] Hallock, K.J.; Lee, D.K.; Ramamoorthy, A. MSI-78, an analogue of the magainin antimicrobial peptides, disrupts lipid bilayer structure via positive curvature strain. *Biophys. J.* **2003**, *84*, 3052–3060.
- [45] Henzler-Wildman, K.A.; Lee, D.K.; Ramamoorthy, A. Mechanism of lipid bilayer disruption by the human antimicrobial peptide LL-37. *Biochemistry* **2003**, *42*, 6445–6558.
- [46] Pozo Navas, B. ; Lohner, V.; Deutsch, G.; Sevcsik, E.; Riske, K.A.; Dimova, R.; Garidel, P.; Pabst, G. Composition dependence of vesicle morphology and mixing properties in a bacterial model membrane system. *BBA-Biomembranes* **2005**, *1716*, 40-48.
- [47] Epand, R. M.; Epand, R. F. Bacterial membrane lipids in the action of antimicrobial agents. *J. Pept. Sci.* **2011**, *17*, 298-305.
- [48] Ulvatne, H. ; Haukland, H.H.; Olsvik, Ø.; Vorland, L.H. Lactoferricin B causes depolarization of the cytoplasmic membrane of *Escherichia coli* ATCC 25922 and fusion of negatively charged liposomes. *FEBS Lett.* **2001**, *492*,62-65.
- [49] Daugelavičius, R.; Bakiene, E.; Bamford, D.H. Stages of polymyxin B interaction with the *Escherichia coli* cell envelope. *Antimicrob. Agents Ch.* **2000**, *44*, 2969-2978.
- [50] Peschel, A.; Sahl, H.G. The co-evolution of host cationic antimicrobial peptides and microbial resistance. *Nat. Rev. Microbiol.* **2006**, *4*, 529–536.
- [51] Rubinchik, E.; Schneider, T.; Elliott, M.; Scott, W.R.P.; Pan, J.; Anklin, C.; Yang, H.; Dugourd, D.; Müller, A.; Gries, K.; Straus, S.K.; Sahl, H.G.; Hancock, R.E.W. Mechanism of action and limited cross-resistance of new lipopeptide MX-2401. *Antimicrob. Agents Ch.* **2011**, *55*, 2743-2754.
- [52] Gifford, J.L.; Hunter, H.N.; Vogel, H.J. Lactoferricin: a lactoferrin-derived peptide with antimicrobial, antiviral, antitumor and immunological properties. *Cell. Mol. Life Sci.* **2005**, *62*, 2588–2598.
- [53] Epand, R.F. ; Pollard, J.E.; Wright, J.O.; Savage, P.B.; Epand, R.M. Depolarization, bacterial membrane composition, and the antimicrobial action of ceragenins. *Antimicrob. Agents Ch.* **2010**, *54*, 3708-3713.

- [54] Cheng, J.T.J.; Hale, J.D.; Elliott, M.; Hancock, R.E.W.; Straus, S.K. The importance of bacterial membrane composition in the structure and function of aurein 2.2 and selected variants. *BBA-Biomembranes* **2011**, *1808*, 622-633.
- [55] Zhao, H.; Sood, R.; Jutila, A.; Bose, S.; Fimland, G.; Nissen-Meyer, J.; Kinnunen, P.K.J. Interaction of the antimicrobial peptide pheromone Plantaricin A with model membranes: Implications for a novel mechanism of action. *BBA-Biomembranes* **2006**, *1758*, 1461-1474.